RESEARCH PAPER

Structural Control Effect and Performance of Structure Under Control of Impulse Semi-active Mass Control Mechanism

Ming-Hsiang Shih[1] · Wen-Pei Sung[2]

Abstract

In this article, a new semi-active damper is proposed to reduce the structural displacement and the maximum roof displacement responses of buildings under dynamical excitation. The main feature of such a semi-active mass damper is that it has a high natural frequency relative to conventional mass dampers and that it will only perform negative work on the structure based on the direction of motion of the structure and the control mass. This proposed damper contains a coupling mechanism that uses a small amount of driving force to change the "release" and "capture" states between the control mass and the structure. A mathematical model and the control logic of this proposed method are derived and discussed to compare the structural responses of the structure under various control parameters. Then, a parameter study is conducted to discuss the optimal design parameters for this proposed mass damper. The optimal design parameters for this proposed mass damper are as follows: frequency ratio around 4 with a mass ratio around 0.04–0.06, and suitable mass distribution at each floor. This proposed mass damper achieves constructive shock absorption effects to reduce structural displacement and maximum roof displacement.

Keywords Semi-active mass damper · Frequency ratio · Mass ratio · Mass distribution · Structural displacement · Maximum roof displacement

1 Introduction

Theoretically, to design a safe structure, three requirements, namely, correct load data, correct material strength, and correct design and analysis, must be met. After the structure is completed, it will be affected by external loads such as wind and earthquakes. Construction quality, construction techniques, and properties of building materials are assumed in the design stage, so the data used in this stage are not necessarily correct. The analysis model only provides a reasonable assumption and does not represent the real structure after completion. To meet structural safety requirements,

the structural design considers appropriate safety factors. Recently, progress in science and sophisticated research achievements have allowed fairly reliable data on load characteristics to be obtained. In addition, advances in materials science have provided new construction materials that improve the strength and predictability of said materials, while innovations in computer technology and analytical methods for structural design (MasterSeries 2019; Sap 2000 2019; STAAD 2019; RISA-3D 2019; ETABS 2019; SkyCiv Structural 3D 2019) have made previous concepts obsolete. Many high-rise buildings, towers (Citigroup Center 1976; Taipei 101 2004; CN Tower 1976; John Hancock Tower 1976; Ellen Lupton 1993) and long-span bridges (List of longest suspension bridge spans 2019) have been built in response to human needs.

Such structures are relatively flexible and have lower damping, so designers must consider several factors: safety, comfort, and functionality. First, due to the small cross-section of such structures, external forces can lead to large displacement, which can cause structural failure. Second, large structural displacement and acceleration can cause great discomfort to the users. Third, large structural

✉ Wen-Pei Sung
wps@ncut.edu.tw

Ming-Hsiang Shih
iloveaachen@gmail.com

[1] Department of Civil Engineering, National Chi-Nan University, Pu-Li 545, Nan-Tou, Taiwan

[2] Department of Landscape Architecture, Integrated Research Center for Green Living Technologies, National Chin-Yi University of Technology, Taichung 41170, Taiwan

displacements can degrade the functionality of a structure such as a high-tech plant. To solve the above problems, certain materials can be used to enhance the safety factors. However, the use of such materials may not be cost-effective. Therefore, to meet economic requirements and comply with safety requirements while making breakthroughs in building height restrictions, many structural control methods have been developed. Many famous structures have been built using new techniques and designs. One such approach is to use control theory, which involves changing the behavior of a system with minimal energy. Structural control is achieved by applying the minimum control force to change structural characteristics such as mass, stiffness, and damping. The objective of structural control is to minimize structural responses under external loads.

The two current types of control are passive control and active control. The first, passive control (Basharkah and Yao 1982; Choi et al. 2008; Chen et al. 2010; Jung et al. 2010; Murase et al. 2013; Zhang and Balendra 2013; Cacciola and Tombari 2015) requires no external energy supply. The control force of passive control is derived from the potential energy of structural deformation, such as retrofitting of structures with tuned mass dampers that have a frequency similar to that of the structure or non-elastic bracing elements at inter-stories. The disadvantage of passive control is that such approaches provide insufficient strength to counter large deformation. Because such approaches change the structural characteristics only slightly, the control effect is somewhat limited. The second, active control (Fisco and Adeli 2011; Liu et al. 2011, 2013; Zeng et al. 2014), requires a supply of external energy to exert a control force. An active control system must be ready to detect structural responses according to predetermined control laws, transmit a control signal, and output commands to the system to produce a moderate control force. Common active control methods are optimal control, pole assignment, and modal control.

A recently emerging research direction is semi-active control (Shih et al. 2002; Shih and Sung 2010; Palacios-Quiñonero et al. 2012; Hiramoto et al. 2014; Shih and Sung 2014). Semi-active control and passive control share some similarities. The control power of these two control methods is derived from the vibrations of the structure to be controlled. The main characteristic of semi-active control is that the control force, which is provided with local adaptability to the structure, can be changed based on the requirement of structural control. Semi-active control can achieve the maximum vibration control capability using the minimum control energy. Therefore, the main difference between semi-active control and active control is the low control energy requirement. The power demands of a semi-active control system are not prohibitive and can be provided by a home-type uninterruptible power system in the event of an earthquake.

A new structural control method, a semi-active mass control mechanism is proposed in this research. The semi-active damper adopts the advantages of a tuned mass damper (TMD) and an active mass damper to improve the control effect. This semi-active mass control mechanism does not require a power supply. The actions of this control method are only the acts of capture and release between the structure and the control mass. The "releasing" and "capturing" actions are determined by the structural response to the external excitation. Since this action changes the natural frequency of the entire structure, the dynamic response of the structure can be greatly reduced.

In this paper, a mathematical model and the control law of this semi-active control mechanism are presented. Then the differences between the maximum displacement ratio of the structure and control mass, the maximum control force exerted by the control mass, and the control power exerted on the structure under tuned mass damper control and the proposed semi-active mass damper are compared. The parameter study of this proposed method is discussed and compared with those of structures without control and with a TMD to obtain the optimal design parameters of this proposed semi-active damper. In this paper, the advantages and disadvantages of various mass dampers are evaluated by comparing the change in the roof displacement response and the change in the base shear response in a 3 degree-of-freedom (3-DOF) structure.

2 Methodology for Impulse Semi-active Mass Damper, ISAMD

The proposed Impulse Semi-Active Mass Damper (ISAMD) is based on the principle of the tuned mass damper and mitigates its defects. Thus, the working principle of the tuned mass damper is briefly discussed, and the actuation principle and mechanical behavior of the ISAMD are explained in the next section. Figure 1a is bare structure, Fig. 1b is the structure under control of TMD, and Fig. 1c is the structure with ISMAD. The main difference between Fig. 1b, c is that the active joint is installed between TMD and structure.

2.1 Working Principle of the Tuned Mass Damper

The tuned mass damper is a passive control technology. A mass block whose weight is much less than the weight of structure is installed in a structure and connected to the structure with a spring and a damper, shown in Fig. 1. The oscillation system of the mass-spring-damper is similar to the original basic vibration frequency of the structure in the case of a fixed structure. The action principle can be understood from the characteristics of its vibration modes. The mathematical model for n degrees of freedom of a shear
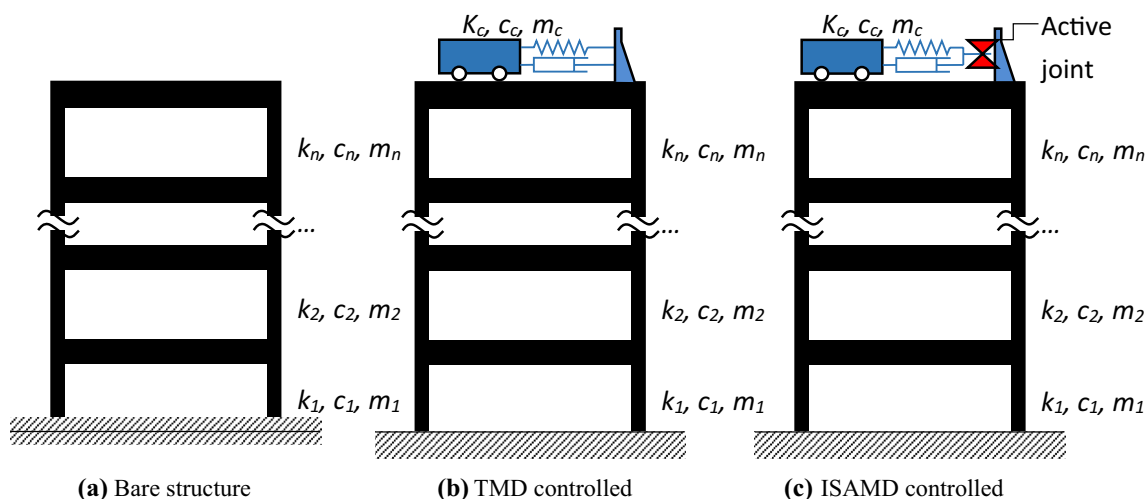
Fig. 1 Structure and mass damper systems in study

structure without a mass damper is expressed in the following equation of motion:

$$\underline{\underline{M}}\ddot{\underline{X}}(t) + \underline{\underline{C}}\dot{\underline{X}}(t) + \underline{\underline{K}}\underline{X}(t) = \underline{P}(t) \tag{1}$$

where $\underline{\underline{M}}$, $\underline{\underline{C}}$, $\underline{\underline{K}}$ are the matrix of structural mass, damping and stiffness, respectively; $\underline{X}(t)$, $\dot{\underline{X}}(t)$, $\ddot{\underline{X}}(t)$ are the response vectors for structural displacement, velocity and acceleration, respectively; $\underline{P}(t)$ is the action vector of external force.

The square root for the eigenvalues of Eq. (1) is the modal frequency for the structure without control, $\omega_1, \omega_2, \ldots \omega_n$ and $\omega_1 < \omega_2 < \cdots < \omega_n$. The corresponding vibration mode vectors are $\underline{\Phi}_1, \underline{\Phi}_2, \ldots \underline{\Phi}_n$. When a tuned mass damper with a mass block m_c, natural frequency ω_c and damping ratio ξ_c is added at the roof of the structure, and the structural system has a degree of freedom, then, the equation of motion can be rewritten as follows:

$$\underline{\underline{M}}^* \ddot{\underline{X}}^*(t) + \underline{\underline{C}} \dot{\underline{X}}^*(t) + \underline{\underline{K}}^* \underline{X}^*(t) = \underline{P}^*(t) \tag{2}$$

where the variable symbols are the same as those in the definition of Eq. (1). The symbol "*" is for the $n+1$ dimensions to separate the original structure without control and the structure under control of the TMD.

When the natural frequency of the TMD ω_c is very close to the fundamental natural frequency of the original structure ω_1, TMD can produce fine modal interaction to perform excellent shock-absorbing effect.

The shock-absorbing effect of the TMD comes not from the increased damping ratio of the system modalities but from the interaction of two similar modal reactions. Therefore, when the ideal condition is not satisfied, such as when the mass ratio of the TMD is larger, the damping ratio cannot be ignored, the frequency of the TMD is not close to

the basic frequency of the structure, or the frequency of the force is not equal to the basic frequency of the structure, the control effect of the TMD is less than the ideal condition. Even an opposite effect may occur; the structural responses of the controlled structure may be greater than those of the uncontrolled structure, as shown in Fig. 2. When the mass ratio of the TMD increases, the aforementioned first and second modal interaction effects no longer exist, so the shock absorption effect of the TMD is smaller.

The above-mentioned loss of the TMD control effect is caused by the frequency of the TMD not being close to the fundamental frequency of the structure, which is known as the "detuning effect." This is the first problem needing to be overcome in this study. The shock absorption effect of the TMD does not increase with its mass ratio, and the result of increasing the mass ratio is not necessarily an improvement. Therefore, the shock absorption effect of the TMD has certain limitations.
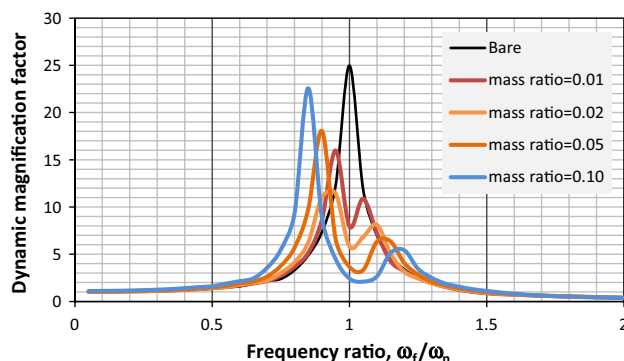

Fig. 2 Response function of the TMD controlled structure with various mass ratios

2.2 Working Principle of Impulse Semi-active Mass Damper

The mass blocks of the TMD are separated from the structure into two systems. Equation (3) describes the relationship of motion equilibrium between the structure and the TMD, as follows:

$$\underline{M}\ddot{X}(t) + \underline{C}\dot{X}(t) + \underline{K}X(t) = \underline{P}(t) + u(t) \tag{3a}$$

$$m_c\ddot{x}_c(t) = p_c(t) - u(t) \tag{3b}$$

$$u(t) = k_c\left[x_c(t) - x_n(t)\right] + c_c\left[\dot{x}_c(t) - \dot{x}_n(t)\right] \tag{3c}$$

where $u(t)$ is the control force of the controlling mass block, acting on its installation position. It also acts in the opposite direction on the control mass block. $p_c(t)$ is an external force acting on a mass block. If the external force is wind, usually $p_c(t) = 0$. If the external force is an earthquake force, then $p_c(t) = -m_c\ddot{x}_g(t)$.

The excellent shock absorption effect of the TMD under an external force with a resonant frequency is derived from the control force produced by the TMD. The movement direction of the TMD is almost always in the opposite direction of that of the structure, so it does the most negative work on the structure and absorbs the greatest energy. Once the frequency of the external force deviates from the resonant frequency and the frequency ratio of the TMD deviates from the optimal frequency ratio, the control mass block has an increased chance of doing positive work on the structure and gradually loses the energy dissipation effect on the structure.

If an active joint is installed between the control mass block and the structure, it can perform "capturing" and "releasing" actions between the control mass block and the structure, as shown in Fig. 1c. When the active joint is in the capturing state, there is an interaction force between the control mass block and the structure due to the deformation of the spring and the motion of the damper. When the active joint is in the releasing state, the interaction force between the control mass block and the structure is only faint friction and can be ignored. Therefore, Eqs. (3a) and (3b) can describe these control forces:

Because the spring between the mass blocks and structural connections is in a free length state, the initial relative displacement should be deducted to calculate the control force.

Two control forces at any time can be selected by Eq. (4). There are two kinds of factors, objective factors and subjective factors that influence the selection of the control force, as follows:

(1) Subjective factors—control purposes.

The primary purpose of structural control is to reduce the displacement, velocity and acceleration responses of the structure, and the weight relationships of these three can affect the choice of the control force. In addition, when considering the installation space of the mass damper, it is possible to choose a control option that slightly sacrifices the shock absorption effect and reduces the displacement of the mass block. Otherwise, the maximum energy dissipation can be taken as a consideration to simply exclude all control forces that will perform positive work on the structure. The control force with the least energy input for the structure is considered for analyzing the energy dissipation effect in this study.

(2) Objective factors—control parameters

Under the control purpose of subjective cognizance, the control effect is affected by the control system parameters, such as the ratio of the mass summation of the control mass blocks to the total mass of the structural system, defined as mass ratio η, and the ratio of the frequency of the control mass block to the natural frequency of the structural system, defined as frequency ratio Ω.

A control law of this damper can be developed to describe the state of the active joint under comprehensive consideration of the subjective and objective factors.

2.3 Control Law of Impulse Semi-active Mass Damper

The control force of this proposed semi-active mass damper has the characteristics of large force and short time duration, so it is named as Impulse Semi-active Mass Damper (ISAMD). The reason for the control force having a short

$$u(t) = \begin{cases} k_c\left[x_c(t) - x_n(t) - d_{r0}\right] + c_c\left[\dot{x}_c(t) - \dot{x}_n(t)\right] & \text{J\_STATUS} = \text{"LOCK"} \\ 0 & \text{J\_STATUS} = \text{"UNLOCK"} \end{cases} \tag{4}$$

where J_STATUS: represents the current status of the active joint. If the active joint executes the "capturing" action, it is in the "LOCK" state; otherwise, J_STATUS is in the "UNLOCK" state. d_{r0} is the relative displacement between the mass blocks and structural connections when the active joint is last converted to the "LOCK" control status.

time duration is explained below. If the control system chooses the maximum energy dissipation, then it can be achieved in two ways:

(1) Zero Positive Force principle

When the action direction of the control force and the structural movement (velocity) at the action point of the control force are the same, the control force does positive work on the structure. At this moment, the direction of the control force or the structural movement needs to be reversed. However, if neither can be reversed, the control force can only be zeroed, such as the second choice of Eq. (4).

(2) Principle of maximum negative power

If the movement direction of the control force and the structural movement of the connection point are opposites, or either of the above is zero, the control force does not add a positive power to the structure. When the active joint is in the "UNLOCK" state and the relative velocity direction of the control mass block to the structure and movement direction of the structure are opposite, the active joint switches to the "LOCK" state to generate a control force of negative work on the structure. This represents a reversal movement of the structure (the velocity is zero and turns to the opposite direction of the previous moment). This is the point at which the active joint switches the connection state to "LOCK." But when the active joint switches to "LOCK," the capability of the control force to do negative work on the structure is decreased, so a better time must be chosen. When the structure returns to zero displacement or zero acceleration, the movement velocity of the structure reaches the local extreme and the movement velocity of the control mass block relative to the structure also reaches the maximum. The state of the active joint returns to the "LOCK" state at this time. This state achieves maximum control and negative power.
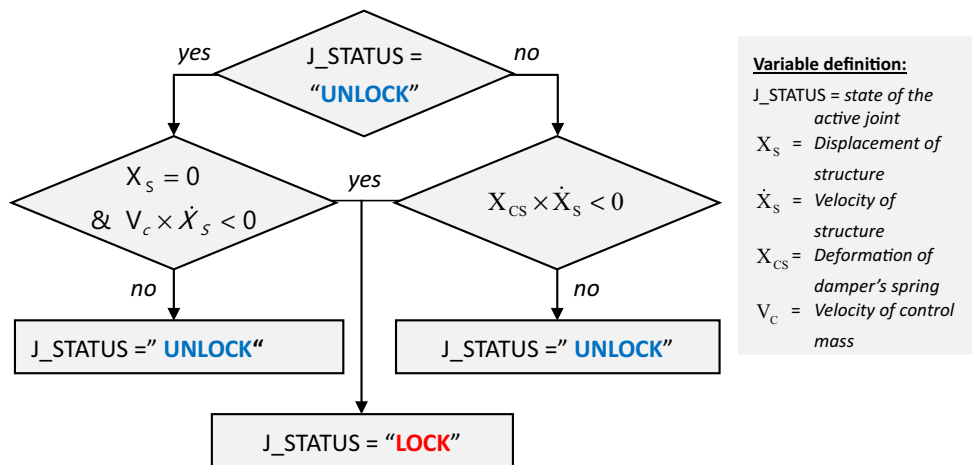
Based on the above two methods, this study develops the following control law to adjust the status of the active joint:

where J_STATUS_i and J_STATUS_{i+1} represent the active joint status for the present and next steps, respectively. X_S is the structural displacement responses at the action point of the control force. $\dot{X}_S$ is the structural velocity responses at the action point of the control force. X_{CS} is the spring elongation response of the damper. V_C is the velocity response of the control mass block.

Figure 3 presents the control flowchart corresponding to Eq. (5). The control law in the control flowchart executes a certain frequency in a digital controller. According to this control law, the active joint is only changed from "UNLOCK" to "LOCK" when the displacement response of the structure is equal to zero; when is approximately one-fourth of the structural fundamental vibration period (or the harmonic external force period), the structural velocity is reversed. Therefore, the active joint must switch to "UNLOCK" before this time point. If the direction of the control force is still opposite to the structural movement at the moment before the velocity of the structure is reversed, the spring with the mass block indicates that the internal force exists. The active joint is switched to "UNLOCK" and the energy of the control spring is released. Although it is the surface of energy dissipation, the control spring does not fully apply its power to shock absorption. Conversely, if the control force changes to zero first and is about to be reversed before the reversal movement of the structure, then the spring performs its shock absorption effect completely, which will be converted to the action of "UNLOCK" for the active joint based on the control law. According to the above discussion, the control force should be reversed within one-fourth of the structural fundamental vibration period so as to obtain a relatively large shock absorption effect. Therefore, this study advocates that the frequency of the control mass

$$J\_STATUS_{i+1} = \begin{cases} LOCK & \begin{cases} \text{if } J\_STATUS_i = LOCK \ \& \ X_{CS} \cdot \dot{X}_S < 0 \\ \text{if } J\_STATUS_i = UNLOCK \ \& \ X_S = 0 \ \& \ V_C \cdot \dot{X}_S < 0 \end{cases} \\ UNLOCK & \text{otherwise} \end{cases} \tag{5}$$

Fig. 3 Control law of impulse semi-active mass damper

should be set at more than twice the fundamental frequency of the structural. In this study, the proposed control technology is called the Impulse Semi-active Mass Damper because the duration of the control force is obviously shorter than the structure period.

3 Analysis Results and Discussion of Control Effects Under Different Control Situations

A single-degree-of-freedom (SDOF) structure and a three-degree-of-freedom (3DOF) structure in the forms of (1) a bare structure, (2) a structure under control of the impulse semi-active mass damper (ISAMD), and (3) one under control of a tuned mass damper (TMD) under excitation of a simple harmonic load and an earthquake force were executed to compare and analyze the structural displacement responses and the displacement responses of the control mass, and to summarize a better combination of control parameters for the ISAMD.

3.1 Structural Responses of SDOF

3.1.1 Comparison of the Control Behavior of Structure Under Control of the TMD and ISAMD

The time histories of the control force and power of the control force of the SDOF structure under excitation of an earthquake load are compared to examine the structural responses of the structure under control of the TMD and the ISAMD. Assuming that mass of structure $= 1$, stiffness $= 4\pi^2$, damping ratio $= 0.03$, this structure is under control of the TMD and ISAMD. The parameters of the control system are listed as follows:

- TMD: mass of structure $= 0.04$, stiffness of spring $= 0.16\pi^2$, damping ratio $= 0.03$;
- ISAMD: mass of structure $= 0.04$, stiffness of spring $= 2.56\pi^2$ (frequency ratio $= 4$), damping ratio $= 0.0$.

Seismic disturbance, the El-Centro 1940 seismic record, was applied to structures under these two control systems. The time histories of the roof velocity response, control force, control power and cumulative dissipation energy of the structure were plotted from the dynamic analysis results, as shown in Figs. 4 and 5. The control power figure in Fig. 4c shows that the control power from TMD executed positive work on the structure in the first 5–6.5 s, and several other times. Therefore, its energy dissipation effect was adversely affected. The typical time histories of the control force, control power and cumulative dissipation energy of the structure in Fig. 5 are the same as those of the structure with ISAMD control under the same external excitation as Fig. 4. In this

case, the vibration frequency of the mass block is 4 times the fundamental vibration frequency of the structure. Figure 5 shows that the ISAMD only performs negative work on the structure and obtains the maximum energy dissipation effect. Nevertheless, the action mode of the ISAMD is similar to that of the impact force; the value of the control force is four times greater than that of the TMD. This feature should be noted in the mechanism design.

3.1.2 The Control Effect Comparison of the Structure with ISAMD or TMD Under Harmonic Load

This proposed system has two main design parameters: η, which is the ratio of the mass summation of the control mass blocks to the total mass of the structural system, and Ω, the ratio of the frequency of the control mass block to the natural frequency of the structural system. To investigate the influence of η and Ω on the control effect, two shear buildings with one and three degrees of freedom, respectively, were used to verify the seismic proof capability of this proposed system. The analysis results of the SDOF structure with various control situations under harmonic load are discussed in this section to clarify the influence of the design parameters on the control effect and to understand the mechanism of its influence. In this study, the external force frequency ratio β is defined as the ratio of frequency of a periodic load to the natural frequency of the structure. The single DOF building without control (bare structure), with TMD control, $\Omega = 1$, damping ratio $\xi_c = 0.05$ and mass ratios of $\eta = 0.01$–0.10, and with ISAMD control, $\Omega = 1$–8, without damping and with mass ratios of $\eta = 0.01$–0.10 under excitation of various β are compared with the steady state reaction and the relationship of the amplification factor to β. Parameters of structure and control systems are listed in Table 1.

The analysis results of the dynamic magnification factor for the structure without control and those with the TMD and SAMD control are presented in Fig. 6. Figure 6 shows that shock absorption of the TMD provides excellent seismic proof capability at the resonance frequency. But two peaks before and after the resonance frequency result in an unsatisfactory control effect. Major shortcomings of the structure under control of the TMD are that a displacement response greater than that of the original structure may occur when the structure frequency is untuned to the mass sub-frequency or the external force frequency is not in the design of the common frequency ratio. This is called the detuning effect. Regardless of the mass ratio of the ISAMD, the ISAMD provides a very good shock absorption effect without the detuning effect. In contrast, the dynamic magnification factor of the ISAMD, shown in Fig. 6, displays only a solid line curve. The seismic proof effect is almost the same as that of the smaller $\eta(0.01)$ to the larger $\eta(0.1)$. The frequency ratio Ω of the ISAMD is 4.0. It is noteworthy that the relationship

Fig. 4 Roof velocity, control force, control power and accumulated work of the TMD system under seismic excitation

(a) Roof velocity of structure

(b) Control force

(c) Control power

(d) Accumulated work
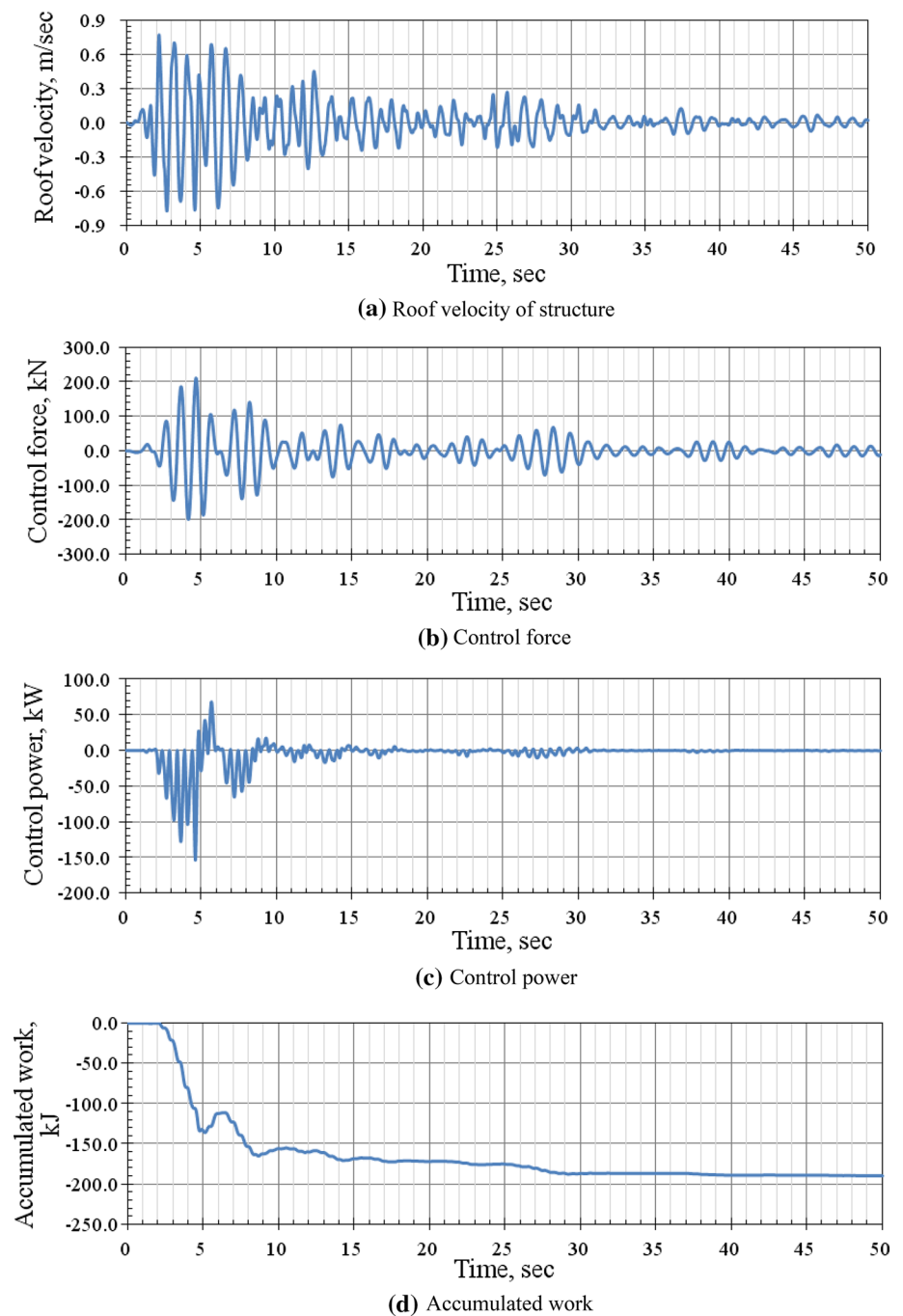
between the dynamic amplification factor and the external force frequency of the ISAMD is very flat and remains almost entirely below 2. The dynamic magnification factors for the external force frequency ratio β between 0.5 and 1.2 are significantly smaller than those of the original structure, providing an excellent shock absorption effect. Figure 6 clearly shows that the SDOF structure with the TMD becomes a two-degrees-of-freedom structure in this situation. The dynamic magnification factor curve has two peaks, regardless of the η, and the horizontal distance of the two peaks is magnified with

an increase in mass ratio. The control effect of the structure under control of the TMD fades as the η increases. In contrast, the dynamic magnification factor curve of the structure under control of the ISAMD shows that it has no apparent dynamical phenomena or that there is no apparent frequency response, because the overall structure under control of the ISAMD is a variable system. Therefore, there is no clear peak of reaction in the structure under control of the ISAMD. Furthermore, to understand the influence of the control mass ratio on the control effect of the passive control-tuned mass

Fig. 5 Roof velocity, control force, control power and accumulated work of the ISAMD system under seismic excitation
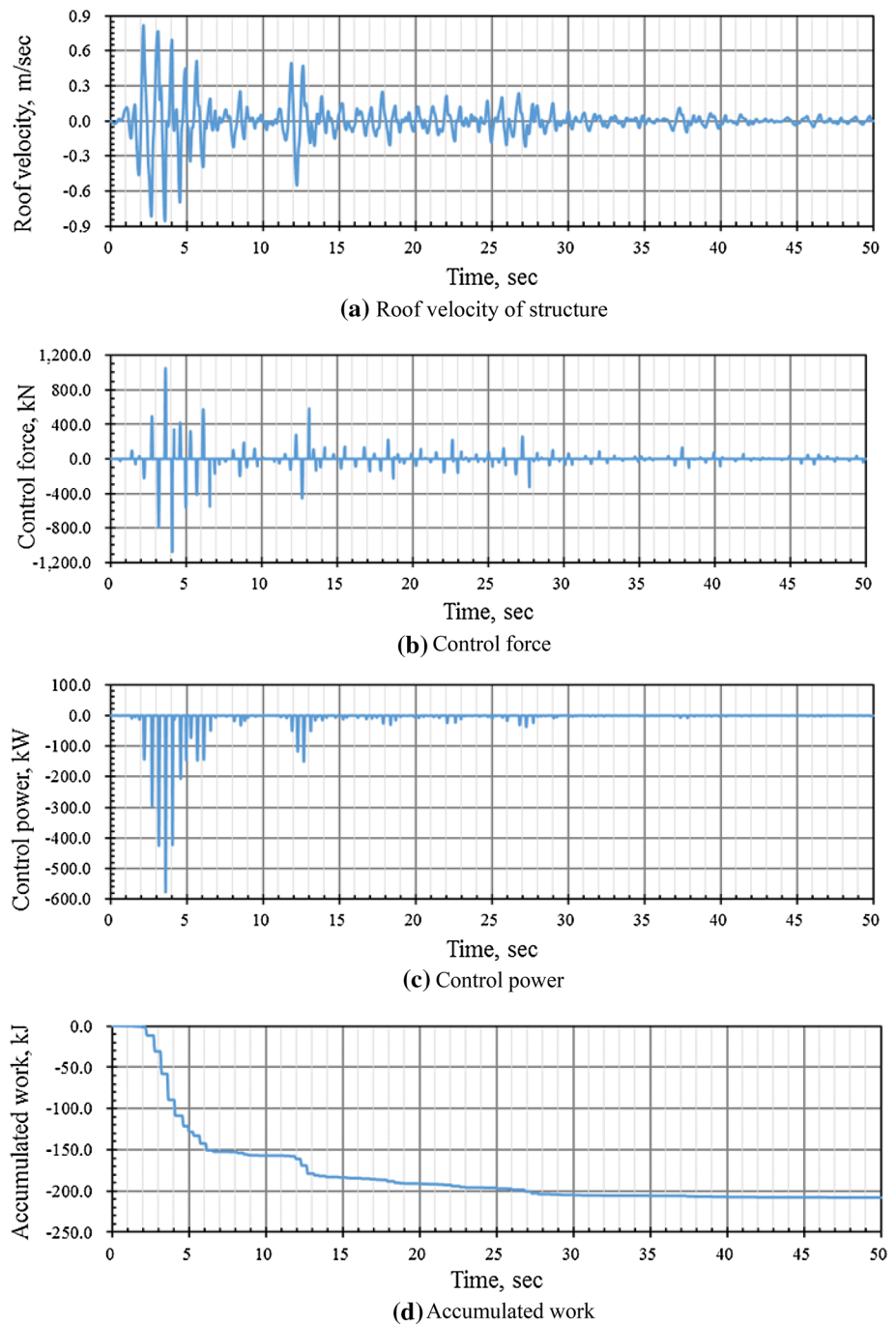

(a) Roof velocity of structure

(b) Control force

(c) Control power

(d) Accumulated work

Table 1 Parameters of structure and control systems

Bare structure	$\omega_n = 1$ Hz, $\xi = 0.03$
TMD controlled	Mass ratio $\eta = 0.01, \ 0.02, \dots 0.10$ Damping ratio $\xi_c = 0.05$ Frequency ratio $\Omega = 1$
ISAMD controlled	Mass ratio $\eta = 0.01, \ 0.02, \dots 0.10$ Damping ratio $\xi_c = 0.0$ Frequency ratio $\Omega = 1, \ 2, \dots 8$

damper, the TMD and this proposed ISAMD, three dimensions for the dynamic magnification factor variation of the TMD with a frequency ratio of 1.0 and damping ratio of 0.05 are shown in Fig. 7, and those of the ISAMD with mass ratios of 0.01 and 0.04 are shown in Fig. 8. Figure 7 reveals the variation in the dynamic magnification factor of the structure under the TMD control with $\Omega = 1$, when subjected to periodic loads of $\beta = 0.0$–2.0. Figure 8 shows the variation in the dynamic magnification factor of the structure under the ISAMD control with mass ratio of 0.01 and 0.04 and
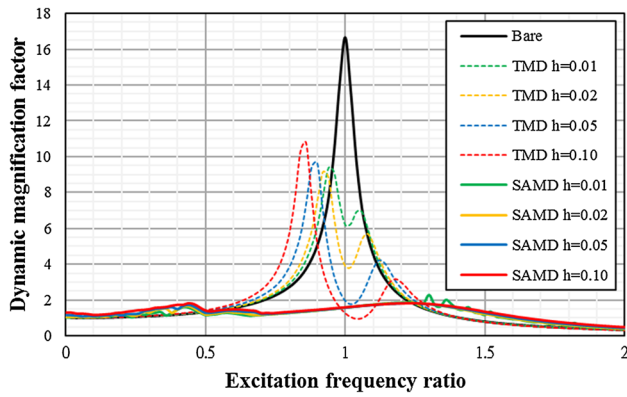
Fig. 6 Dynamic amplification factor of SDOF under TMD with $\Omega = 1.0$, $\xi_c = 0.05$, and ISAMD with $\Omega = 4.0$
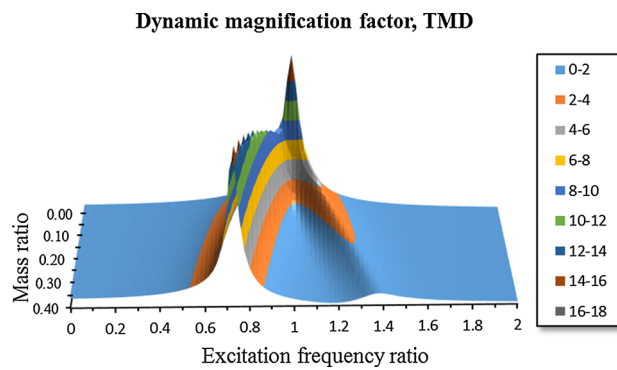

Fig. 7 Amplification surface of SDOF under TMD, $\Omega = 1.0$, $\xi_c = 0.05$

Fig. 8 Dynamic magnification factor of SDOF under ISAMD with $\eta = 0.01$ and $\eta = 0.04$

various frequency ratios, when subjected to periodic loads of $\beta = 0.0$–2.0, respectively. Figures 9 and 10 show the amplification level surface of the SDOF under ISAMD control with frequency ratios of 4 and 8 when subjected to periodic loads of $\beta = 0.0$–2.0, respectively.

Figure 7 shows that the control effect of the TMD cannot be simply improved by increasing the mass ratio, for a mass ratio above 0.05 no longer has a clear shock absorption effect. Figure 8 displays the influence of different control frequency ratios on the dynamic magnification factor for mass ratios of the ISAMD between 0.01 and 0.04; good shock proof capability at the control frequency ratio is greater than or equal to 3. This study suggests that the control frequency ratio of the ISAMD should be 3–5 because a higher control frequency ratio leads to an extremely large control force and mass displacement response. In addition, Figs. 9 and 10 reveal that if the mass ratio is very small, the control effect of the ISAMD is essentially independent of the mass ratio. Although the dynamic magnification factor slightly fluctuates with a larger mass ratio, it is still very small. The control effect cannot be deduced entirely
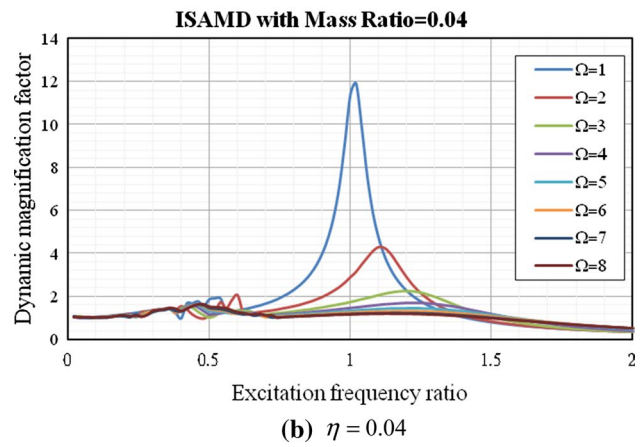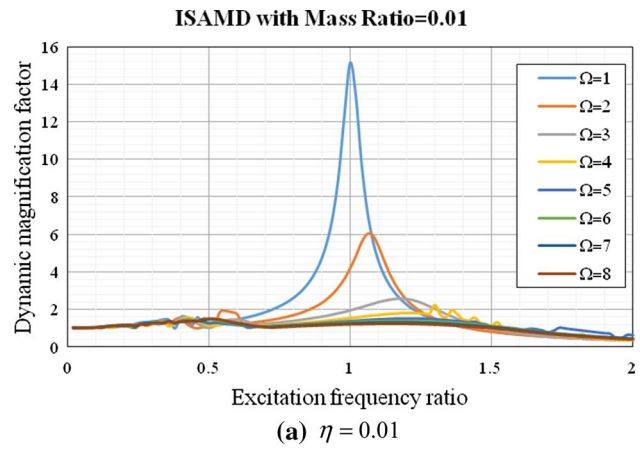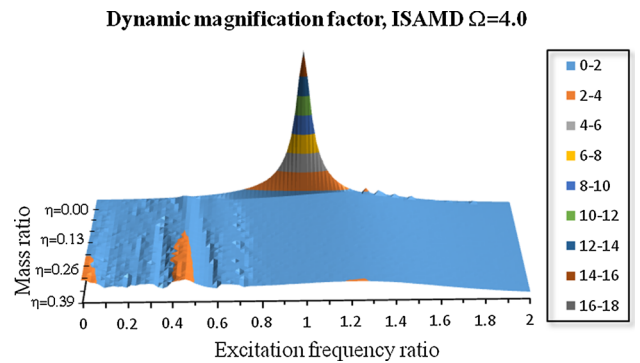

Fig. 9 Amplification level surface of SDOF under ISAMD control, $\Omega = 4$

from the analysis results of the structure under excitation of harmonic load because of the wide frequency band of seismic force. Figures 9 and 10 show that a high mass ratio does not have an adverse effect on the structure with the ISAMD. The mass ratio may be improved to promote the shock absorption effect for a structure with the ISAMD under excitation of seismic loading.
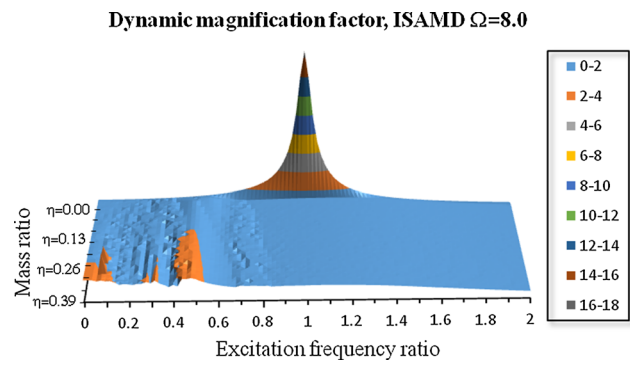
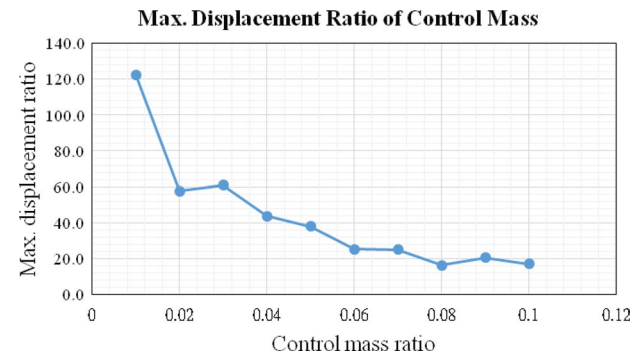**Fig. 10** Amplification level surface of SDOF under ISAMD control, $\Omega = 8$

Fig. 11 The maximum displacement ratio of the control mass for ISAMD control, $\Omega = 4$

Table 2 Structural parameters of 3DOF model

Floor	Mass tn	Stiffness (kN/m)	Damping coefficient (kN s/m)
1	100	19,932.327	63.447
2	100	19,932.327	63.447
3	100	19,932.327	63.447

Table 3 Modal properties of 3DOF model

Property	Mode-1	Mode-2	Mode-3
Frequency, rad (s)	6.28319	13.79360	28.80305
Mode shape	1.00000	1.00000	1.00000
	1.80194	1.04545	-2.16216
	2.24698	0.09297	3.67494
Damping ratio	0.01000	0.02195	0.04584

Table 4 Parameter settings of control system

Control type	Mass ratio	Frequency ratio	Damping ratio
TMD	0.01, 0.02,… 0.15	0.947[a]	0.0726[a]
ISAMD	0.01, 0.02,… 0.15	2, 4,…10	0.00, 0.01, 0.02, 0.5

[a]Optimized

Figure 11 displays the relationship of the ratio of the maximum displacement responses of control mass and the control mass ratio for the control mass under excitation of harmonic loading with a resonance frequency with a frequency ratio of 4.0. The maximum displacement response ratio of the mass block is defined as the ratio of the maximum displacement of the mass block to that of the uncontrolled structure at resonance. Figure 11 reveals that the maximum displacement response of the mass block monotonically decreases with increasing mass ratio. When the mass ratio is 0.01, the mass displacement may be greater than the resonant displacement of the bare structure. The maximum displacement of the mass block can be controlled within a reasonable range by choosing a larger mass ratio.

3.2 Structural Responses of 3DOF Structure

3.2.1 Comparison of the Control Behavior of the Structure Under Control of the TMD and ISAMD

To verify the seismic proof capability of this proposed mechanism, a 3DOF structure was subjected to the forces of a near-field earthquake. A combination of El Centro ground motions with simple pulses was used to simulate the near-fault features of the structure under control of the TMD and ISAMD. The structural parameters and modal properties of this 3DOF model are listed in Tables 2 and 3, respectively. This 3DOF building was tested without control, with TMD control, $\Omega = 0.947$ (optimized) and damping ratio $= 0.0726$ (optimized), and with ISAMD control $\Omega = 2, 4, 6, 8, 9$ and 10 with ratios of mass variation of $\eta = 0.01, 0.02, 0.03, 0.04, 0.05, 0.06, 0.07, 0.08, 0.09, 0.10, 0.11, 0.12, 0.13, 0.14$ and 0.15 and damping ratio $= 0.00, 0.01, 0.02$ and 0.5. All parameter settings of the TMD and ISAMD systems are listed in Table 4. Figure 12 displays the time history of roof displacement responses of the structure under excitation of seismic force for the bare structure, structure under TMD control with a mass ratio of 0.04, the optimized frequency ratio of 0.947, and the optimized damping ratio of 0.0726, and structure under ISAMD control with mass ratio of 0.04 and frequency ratio of 4.

Figure 13 reveals the trend of the maximum roof displacement of the structure under TMD control with mass ratios of 0.01–0.15, the optimized frequency ratio of 0.947, and a resonance frequency ratio of 1.0. Figure 14 displays the relationship curve of the maximum roof displacement
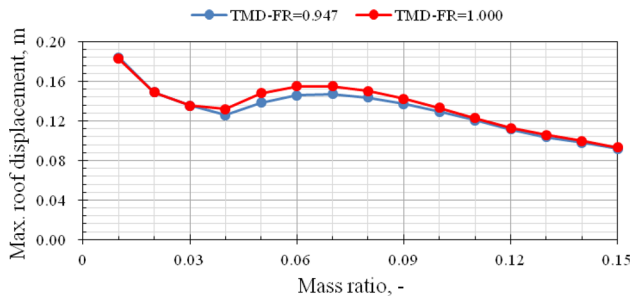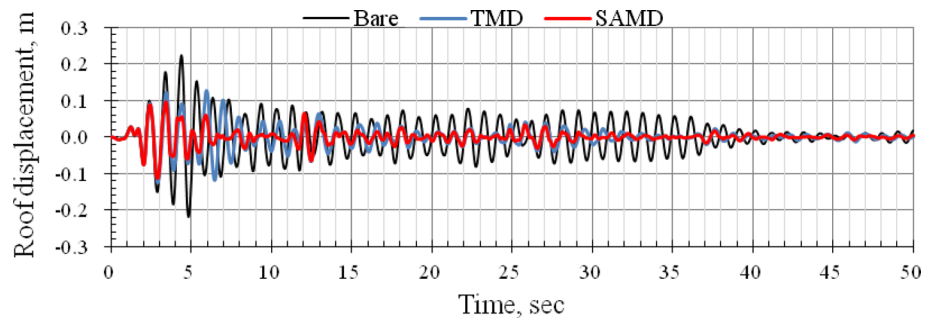
Fig. 12 Time history of roof displacement

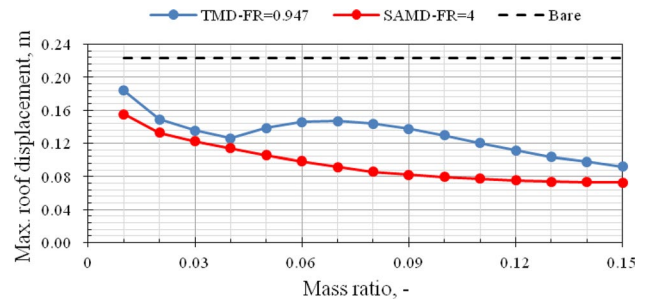**Fig. 13** The maximum roof displacement under control of the TMD with various frequency ratios and mass ratios

Fig. 14 Maximum roof displacement under control of the ISAMD with various frequency ratio and mass ratio

Fig. 15 Comparison of maximum roof displacement of bare, TMD controlled and ISAMD controlled structures
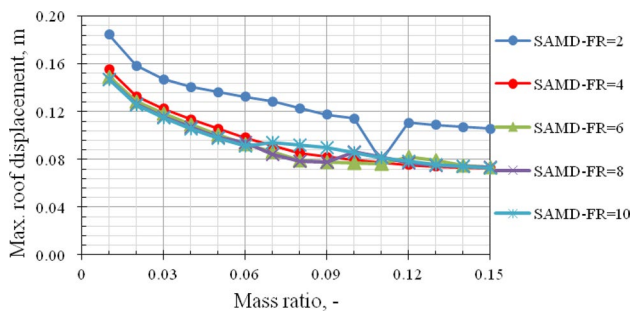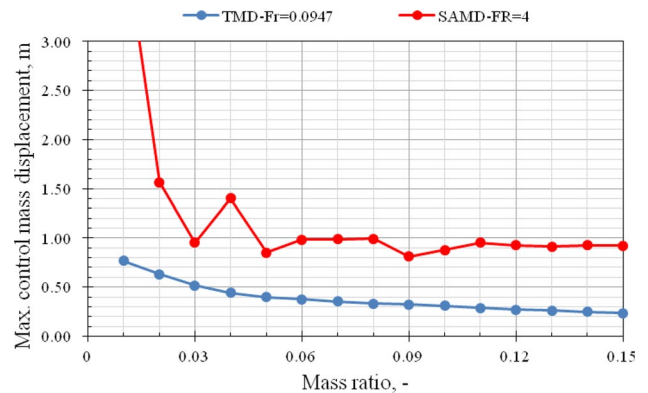

Fig. 16 Comparison of maximum control mass displacement between TMD controlled and ISAMD controlled structures with various mass ratio

of the structure under control of the ISAMD with various frequency ratios and mass ratios. The comparison of the maximum roof displacement of the structure with mass ratio = 0.04 for the bare structure and for the structure under control of the TMD and ISAMD is shown in Fig. 15. Figure 16 presents the comparison of maximum control mass displacement between TMD control and ISAMD control with various mass ratios.

3.3 Parameter Study and Discussion

3.3.1 Influence of η and Ω

Figure 12 shows that the reduction ratio of the maximum roof displacements for the structure under TMD and ISAMD

control are 43% and 49%, respectively. The shock absorption effect of the structure under ISAMD control is only slightly better than that of the TMD. Figure 13 shows that the control effect of the structure under TMD control increases with increases in the mass ratio. Nevertheless, fluctuation occurs when the mass ration is less than 0.07. The reason is that the values of the optimized frequency ratio and damping ratio are estimated for mass ratio = 0.04. Therefore, the control effect increases with the mass ratio when the mass ratio is less than 0.04, but it decreases with increases in mass ratio. Then the control effect rises with increasing mass ratio when

Table 5 Displacement variance and the maximum roof displacement for the structure under TMD control with $\eta = 0.04$

Control type	TMD control										
Item-1	Displacement variance										
$w_1(\%) \because w_2(\%)$	0	10	20	30	40	50	60	70	80	90	100
100	8.98										
90	9.01	9.00									
80	8.90	8.98	8.99								
70	8.65	8.81	8.91	8.94							
60	8.24	8.48	8.66	8.79	8.85						
50	7.72	8.00	8.25	8.46	8.62	8.71					
40	7.14	7.43	7.71	7.98	8.21	8.40	8.52				
30	6.58	6.85	7.13	7.41	7.68	7.92	8.13	8.29			
20	6.06	6.30	6.56	6.83	7.10	7.36	7.61	7.83	8.01		
10	5.59	5.81	6.04	6.28	6.53	6.79	7.04	7.29	7.51	7.71	
0	5.18	5.37	5.58	5.79	6.02	6.26	6.49	6.74	6.97	7.20	7.40
Item-2	Maximum roof displacement										
$w_1(\%) \because w_2(\%)$	0	10	20	30	40	50	60	70	80	90	100
100	6.07										
90	5.74	5.66									
80	5.81	5.82	5.74								
70	5.54	5.70	5.78	5.79							
60	5.07	5.31	5.51	5.65	5.72						
50	4.93	4.95	5.02	5.25	5.44	5.58					
40	4.96	4.95	4.93	4.95	4.97	5.18	5.36				
30	5.03	5.00	5.00	4.98	4.93	4.95	4.97	5.09			
20	5.15	5.12	5.08	5.03	5.01	4.98	4.93	4.95	4.97		
10	5.22	5.21	5.20	5.16	5.11	5.04	5.01	4.95	4.93	4.95	
0	5.24	5.25	5.26	5.25	5.23	5.19	5.13	5.04	4.97	4.91	4.93

Comment: $w_1(\%) = (m_1/m) * 100\%, w_2(\%) = [(0 \sim 100\%) - w_1(\%)], w_3(\%) = 100 - w_1(\%) - w_2(\%)$

the mass ratio reaches 0.07. These results reveal that the control effect of the structure under TMD control is affected by the mass ratio and the frequency ratio. If the dynamic properties of the structure are not estimated properly, the control effect of the TMD may fall short of the desired effect.

The analysis results of Fig. 14 are almost the same as those of the parameter study of the SDOF structure under excitation of harmonic load. The control effect of the structure under ISAMD control is poor when the frequency ratio is less than or equal to 2. But the structure under ISAMD control performs better when the frequency ratio is greater than 3, and the relationship between the frequency ratio and its effect is not strong. A high frequency leads to more control force responses, resulting in impact responses. This phenomenon must be avoided. Thus, a frequency ratio of 3–5 should be recommended in this kind damper. In addition to the frequency ratio of 2, the shock absorption ratio of the structure under ISAMD control increases with increasing mass ratio monotonically. This conclusion is different from

that of the SDOF structure under harmonic load, and it is noteworthy.

Figure 15 shows that the control effects of the structure under ISAMD control are superior to those of the TMD. The control effect of the ISMAD is monotonic and has no relevance to the frequency ratio. Thus, the ISAMD design is simple. Even if the estimation of the dynamic properties of the structure is wrong, the control effect of the ISAMD does not greatly violate expectations. A greater maximum displacement of the control mass leads to greater restrictions of the installation space of the control system. Therefore, the maximum displacement of the control mass is an important factor in comparing the control effects of the TMD and ISAMD. Figure 16 shows that the maximum displacement of the control mass of the ISAMD is greater than that of the TMD. When the mass ratio is greater than or equal to 0.02, the maximum displacement of the control mass of the ISAMD is about 2–4 times that of the TMD. Therefore, the ISAMD is not suitable if installation space is lacking. If

Table 6 Displacement variance and the maximum roof displacement for the structure under TMD control with $\eta = 0.06$

Control type	TMD control										
Item-1	Displacement variance										
$w_1(\%) \therefore w_2(\%)$	0	10	20	30	40	50	60	70	80	90	100
100	8.96										
90	8.90	8.97									
80	8.38	8.68	8.84								
70	7.54	7.96	8.32	8.57							
60	6.65	7.07	7.49	7.88	8.18						
50	5.86	6.23	6.62	7.01	7.38	7.71					
40	5.18	5.49	5.83	6.18	6.54	6.89	7.22				
30	4.63	4.88	5.16	5.46	5.77	6.10	6.42	6.73			
20	4.22	4.40	4.62	4.86	5.12	5.40	5.69	5.98	6.27		
10	3.91	4.05	4.20	4.39	4.59	4.82	5.06	5.32	5.58	5.85	
0	3.71	3.80	3.91	4.04	4.19	4.36	4.55	4.76	4.99	5.22	5.47
Item-2	Maximum roof displacement										
$w_1(\%) \therefore w_2(\%)$	0	10	20	30	40	50	60	70	80	90	100
100	5.61										
90	5.63	5.71									
80	5.01	5.34	5.55								
70	5.03	4.96	4.95	5.22							
60	5.14	5.09	5.05	4.94	4.95						
50	5.29	5.26	5.19	5.09	5.02	4.92					
40	5.31	5.33	5.33	5.29	5.20	5.05	4.93				
30	5.24	5.30	5.34	5.36	5.34	5.28	5.16	4.99			
20	5.11	5.20	5.27	5.32	5.35	5.35	5.32	5.24	5.10		
10	4.94	5.03	5.12	5.20	5.27	5.32	5.34	5.33	5.27	5.17	
0	4.75	4.83	4.93	5.03	5.12	5.20	5.26	5.30	5.31	5.28	5.20

Comment: $w_1(\%) = (m_1/m) * 100\%, w_2(\%) = [(0 \sim 100\%) - w_1(\%)], w_3(\%) = 100 - w_1(\%) - w_2(\%)$

installation space is not limited, the shock absorption effect is the most important consideration in structural design; the shock absorption effect of the structure under ISAMD control is superior to that of the structure under TMD control.

3.3.2 Influence of Mass Distribution

The distributions of the control mass of these 3DOF (m_1, m_2, m_3) are defined as $m_1 = 0 \sim 1$ for the first floor, $m_2 = (0 \sim 1) - m_1$ for the second floor, and $m_3 = 1 - m_1 - m_2$ for the third floor to discuss the influence of the shock absorption effect of this proposed mechanism. To compare the control effects of the structure without control with those of the structure with TMD and ISAMD control with the best design parameters, $\Omega = 1$ for TMD control and $\Omega = 4$ for ISAMD control, with various control mass distributions, a 3DOF structure with $\eta = 0.04$ and 0.06 under excitation of the EL Centro earthquake record was executed to obtain the variation of the structural displacement and the maximum roof displacement

of this structure with different control conditions and mass distributions. The variations of structural displacement and the maximum roof displacement of the structure with TMD control with $\eta = 0.04$ and 0.06 and various mass distributions under excitation of the El Centro earthquake record are listed in Tables 5 and 6, respectively. The variations of the structural displacement and the maximum roof displacement of the structure with semi-active control with $\eta = 0.04$ and 0.06 and various mass distributions under the same excitation are listed in Tables 7 and 8, respectively.

3.3.3 Influence of Mass Distribution

The results in Tables 5 and 6 show that under TMD control, the structure achieves a good control effect for the variation of the roof structural displacement for the control mass concentrated at the top level. Nevertheless, this phenomenon for the maximum roof displacement does not exist under such control, as shown in Table 5. The best control effects

Table 7 Displacement variance and the maximum roof displacement for the structure under ISAMD control with $\eta = 0.04$

Control Type	SAMD control										
Item-1	Displacement variance										
$w_1(\%)$ ∴ $w_2(\%)$	0	10	20	30	40	50	60	70	80	90	100
100	5.30										
90	3.52	4.09									
80	3.36	3.85	3.61								
70	2.65	3.01	2.93	3.12							
60	2.06	2.37	2.46	2.85	3.07						
50	2.26	2.08	2.11	2.45	2.67	3.23					
40	2.02	1.82	1.95	1.97	2.27	2.55	3.37				
30	2.13	1.90	1.88	2.07	2.11	2.29	2.63	3.40			
20	1.79	2.08	2.15	1.95	1.71	1.91	2.15	2.73	3.24		
10	2.08	2.01	1.67	1.95	1.82	1.93	1.77	2.08	2.43	3.18	
0	1.78	1.75	1.56	1.82	1.91	2.01	1.97	1.83	2.18	2.32	2.99
Item-2	Maximum roof displacement										
$w_1(\%)$ ∴ $w_2(\%)$	0	10	20	30	40	50	60	70	80	90	100
100	5.59										
90	4.77	4.75									
80	4.54	4.73	4.81								
70	4.32	4.43	4.49	4.64							
60	4.13	4.18	4.25	4.39	4.47						
50	4.00	4.05	4.11	4.17	4.23	4.38					
40	3.87	3.92	3.97	4.03	4.09	4.16	4.57				
30	3.75	3.80	3.85	3.90	3.96	4.02	4.09	4.87			
20	3.64	3.68	3.72	3.77	3.83	3.89	3.95	4.32	4.89		
10	3.67	3.56	3.60	3.65	3.70	3.76	3.82	3.89	3.96	4.88	
0	3.42	3.45	3.49	3.53	3.58	3.63	3.69	3.76	3.82	3.90	4.71

Comment: $w_1(\%) = (m_1/m) * 100\%$, $w_2(\%) = [(0 \sim 100\%) - w_1(\%)]$, $w_3(\%) = 100 - w_1(\%) - w_2(\%)$

for the structure under TMD control are achieved with the control mass distributed on another floor, not concentrated at the roof. However, TMD control with a high mass ratio and control mass concentrated on the roof achieve the best control effects, as shown in Table 6. The results in Tables 7 and 8 show that the influence of the mass distribution on the control effect is more important with ISAMD control than with TMD control. This phenomenon reveals that when a large control mass is concentrated on the roof, this control method can obtain a greater impulse to diminish the roof velocity. The connection between the active control mass and the structure must be released based on the control principle of the control mass block, which performs only negative work on the structure, although the active control mass block still provides control energy. But the structural control capability cannot be fully used to get a constructive control effect. The results in Tables 7 and 8 show that the suitable mass distributions of the control block are 20–30% at the 2nd floor and 80–70% at the roof, respectively. Notably, all

results show that the detuning phenomenon of TMD control does not occur in the structure under control of this proposed system with TMD and ISAMD control.

4 Conclusions

Analysis shows that a structure with the proposed semi-active control mass with suitable design parameters achieves excellent shock absorption effects. Relevant analysis results can be concluded as follows:

1. To obtain the optimal structural control effects, the natural frequency of the structure should be estimated for the design of a structure under TMD control. The frequency of the tuned mass should be in a narrow range of frequency.
2. This proposed mechanism can "capture" and "release" the active control mass based on the direction and veloc-

Table 8 Displacement variance and the maximum roof displacement for the structure under ISAMD control with $\eta = 0.06$

Control type	SAMD control										
Item-1	Displacement variance										
$w_1(\%) \therefore w_2(\%)$	0	10	20	30	40	50	60	70	80	90	100
100	4.73										
90	3.26	3.54									
80	2.62	2.98	3.09								
70	1.95	2.04	2.47	2.96							
60	1.92	1.96	1.96	2.43	3.48						
50	1.68	1.64	1.62	1.82	2.62	2.86					
40	1.72	1.53	1.77	1.70	1.86	2.41	2.86				
30	1.86	1.65	1.42	1.70	1.67	1.76	2.26	2.77			
20	1.70	1.48	1.42	1.63	1.51	1.66	1.83	1.94	2.45		
10	1.64	1.61	1.49	1.42	1.47	1.45	1.47	1.78	1.86	2.26	
0	1.63	1.56	1.47	1.30	1.52	1.45	1.38	1.57	1.99	1.85	1.98
Item-2	Maximum roof displacement										
$w_1(\%) \therefore w_2(\%)$	0	10	20	30	40	50	60	70	80	90	100
100	4.87										
90	4.50	4.49									
80	4.18	4.26	4.37								
70	3.97	4.06	4.15	4.26							
60	3.79	3.86	3.94	4.04	4.75						
50	3.61	3.67	3.75	3.83	4.09	4.77					
40	3.44	3.49	3.56	3.64	3.73	3.84	4.41				
30	3.28	3.33	3.39	3.46	3.54	3.63	3.74	4.22			
20	3.13	3.17	3.22	3.28	3.36	3.44	3.54	3.65	3.77		
10	3.10	3.10	3.09	3.12	3.19	3.26	3.35	3.45	3.56	3.68	
0	3.09	3.08	3.08	3.08	3.08	3.09	3.17	3.26	3.36	3.48	3.60

Comment: $w_1(\%) = (m_1/m) * 100\%, w_2(\%) = [(0 \sim 100\%) - w_1(\%)], w_3(\%) = 100 - w_1(\%) - w_2(\%)$

ity of movement of the structural displacement. It reacts twice each movement cycle.

3. The optimal design parameters for TMD control are Ω of slightly less than 1.0 and $\eta = 0.04$–0.06, with installation on the roof.

4. The optimal design parameters for this ISAMD control mechanism are $\Omega = 3$–5 with $\eta = 0.04$–0.06, and those for mass distribution of the control block are 20–30% at the 2nd floor and 70–80% at the roof.

5. ISAMD control with $\eta = 0.04$–0.06 achieves greater control effects than does TMD control. ISAMD control with such parameters reduces the large structural displacement and maximum roof displacement to promote structural safety.

6. All results of this research show that this proposed method can prevent the detuning phenomenon of the TMD control; therefore, the structural control effects can be ensured.

References

Basharkah MA, Yao JTP (1982) Reliability aspects of structural control, Purdue University, School of Civil Engineering. Structural Engineering (Technical Report) CE-STR, 82-34

Cacciola P, Tombari A (2015) Vibrating barrier: a novel device for the passive control of structures under ground motion. Proc Math Phys Eng Sci 471(2179):20150075

Chen Y, Cao T, Ma L (2010) Structural vibration passive control and economic analysis of a high-rise building in Beijing. Earthq Eng Eng Vib 8(4):561–568

Choi KM, Jung HJ, Lee HJ, Cho SW (2008) Seismic protection of base-isolated building with nonlinear isolation system using

smart passive control strategy. Struct Control Health Monitor 15(5):785–796

Citigroup Center (1976) https://en.wikipedia.org/wiki/Citigroup_Center Accessed 16 July 2019

CN Tower (1976) https://en.wikipedia.org/wiki/CN_Tower. Accessed 16 July 2019

Ellen Lupton: Kritické hledání cesty (1993) http://designreader.org/ellen-lupton-kriticke-hledani-cesty-1993/ Accessed 16 July 2019

ETABS (2019) Integrated analysis, design and drafting of building systems. https://www.csiamerica.com/products/etabs. Accessed 16 July 2019

Fisco NR, Adeli H (2011) Smart structures: part I—active and semi-active control. Sci Iran 18(3A):275–284

Hiramoto K, Matsuoka T, Sunakoda K (2014) Simultaneous optimal design of the structural model for the semi-active control design and the model-based semi-active control. Struct Control Health Monitor 21(4):522–541

John Hancock Tower (1976) https://en.wikipedia.org/wiki/John_Hancock_Tower Accessed 16 July 2019

Jung HJ, Jang DD, Lee HJ, Lee IW, Cho SW (2010) Feasibility test of adaptive passive control system using MR fluid damper with electromagnetic Induction Part. J Eng Mech 136(2):254–259

List of longest suspension bridge spans (2019) https://en.wikipedia.org/wiki/List_of_longest_suspension_bridge_spans. Accessed 16 July 2019

Liu K, Chen LX, Cai GP (2011) Active control of a nonlinear and hysteretic building structure with time delay. Struct Eng Mech 40(3):431–451

Liu K, Chen LX, Cai GP (2013) Active control of buildings with bilinear hysteresis and time delay. Int J Struct Stab Dyn. https://doi.org/10.1142/S0219455413500272

MasterSeries (2019) Integrated structural analysis, design, drafting and detailing software. http://www.masterseries.com/company.aspx. Accessed 16 July 2019

Murase M, Tsuji M, Takewaki I (2013) Smart passive control of buildings with higher redundancy and robustness using base-isolation and inter-connection. Earthq Struct 4(6):649–670

Palacios-Quiñonero F, Rubió-Massegú J, Rossell JM, Karimi HR (2012) Semi-active-passive structural vibration control strategy for adjacent structures under seismic excitation. J Frankl Inst 349(10):3003–3026

RISA-3D (2019) 3D structural engineering software. https://risa.com/p_risa3d.html. Accessed 16 July 2019

Sap 2000 (2019) Integrated software for structural analysis and design. https://www.csiamerica.com/products/sap2000. Accessed 16 July 2019

Shih MH, Sung WP (2010) A design concept of autonomous controller for improving seismic proof capability of semi-active control device. Exp Tech 34(4):20–26

Shih MH, Sung WP (2014) Development of semi-active hydraulic damper as active interaction control device to withstand external excitation. Sadhana Acad Proc Eng Sci 39(1):123–128

Shih MH, Sung WP, Go CG (2002) Development of accumulated semi-active hydraulic damper. Exp Tech 26(5):29–32

SkyCiv Structural 3D (2019) https://skyciv.com/3d-structural-analysis-software-features/. Accessed 16 July 2019

STAAD (2019) Pro, 3D structural engineering software. https://www.bentley.com/en/products/product-line/structural-analysis-software/staadpro. Accessed 16 July 2019

Taipei 101 (2004) https://zh.wikipedia.org/wiki/%E5%8F%B0%E5%8C%97101. Accessed 16 July 2019

Zeng X, Peng Z, Mo LG, Su Y (2014) Active control based on prediction of structural vibration feedback. In: 2014 fifth international conference on intelligent systems design and engineering applications, https://doi.org/10.1109/ISDEA.2014.35

Zhang Z, Balendra T (2013) Passive control of bilinear hysteretic structures by tuned mass damper for narrow band seismic motions. Eng Struct 54:103–111